Influence of inelastic constant-ductility SDOF location versus near-fault records

Shakiba MONFAREDI, Hamed HAMIDI* and Horr KHOSRAVI

Faculty of Civil Engineering, Babol Noshirvani University of Technology, Iran
*Corresponding Author: h.hamidi@nit.ac.ir

ABSTRACT

The unique features and destructive effects of near-fault records are of high interest to many researchers; the issue of the location of structures against these records has received less attention due to the lack of data. Therefore, in this study, the focus is on the effect of the location of the structure vs. causative fault on the amount of damage. To this end, we need enough near-fault records, which can be simulated using the synthetic generation technique due to the lack of real data. Using the fault parameters obtained for the 1999-Kocaeli earthquake, 273 earthquake records were generated by different location coordinates using the theoretical-based Green's function. In order to evaluate the seismic performance of the structures, OpenSEES software was used to carry out 9828 dynamic time-history analyses. The studied structures are SDOF with constant ductility. The records were applied according to the position of the structure against the causative fault and the relevant spectra were drawn as colored contours. The results showed that the location of the maximum responses in the inelastic state is almost the same as in the elastic state, so the critical location can be determined by a simpler elastic analysis; Stations that showed a maximum value at low periods have a larger amplitude, and stations that showed a maximum value at high periods have a higher pulse period. Both the distance and the angle of the SDOF location are influential in determining the location of the more severe failure.

KEYWORDS

SDOF, location of the structure, near-fault, constant ductility, bilinear steel material

1. Introduction

In recent years numerous research has been carried out about constant-ductility SDOF systems [1]–[3]. In this researches, the focus was on the characteristics of near-fault records and their effects on structures response [4] but site orientation were rarely taken into account. Major researches were related to the effect of rotation of ground motions components [5]-[9]. It is obvious that the distance and angle of the structure from fault alignment and location of the epicenter are effective on structural responses. Therefore, an ensemble of 273 records was generated via theoretical-based Green's function technique by using fault rupture parameters derived from Hamidi et al., [10] research for the 1999 Kocaeli earthquake. Accordingly, the effect of site orientation toward earthquake in the form of S_d and S_a contours has been evaluated for constant-ductility inelastic SDOF systems for two ductility ratio $\mu=2$ and $\mu=3$.

2. Methodology

The SDOF system modeled in this paper includes mass, a rigid column with the elastic beam-column element, and a zero-length spring incorporating Steel01 material with elastic-perfectly plastic behavior. For computing responses, two OpenSEES elastic and inelastic code were prepared. Matlab program was used to connect these two OpenSEES codes. In the *elastic* code, the value of yeilding moment M_y defined to be a large number so that it remains linear but in *inelastic* code the M_y value defined variable that changes due to the yielding resistance.

3. Results and Discussion

For investigating the analysis results, some related contours were presented to show S_d and S_a values supporting periods from 1 to 5 sec as well as a specific value of 0.5 sec.

3.1. Investigation of inelastic S_d values

For the purpose of investigating S_d in the inelastic constant ductility status, some contours were drawn for $\mu=2$ and $\mu=3$ statuses. By comparing these contours with that of the elastic contour, it was specified that for periods equal or less than 3sec the maximum value occurred on the right side of the epicenter, and for periods more than 3sec, the location of maximum value occurred in the left side of the epicenter. The location of the maximum value in low periods in three statuses was similar but in higher periods seem different. It was specified that the maximum and minimum values in these three statuses had no significant difference. Generally, the two inelastic statuses had a close trend.

Figure 1 shows the inelastic spectral displacement (S_d) contour for fault-normal records (for the case μ=3).

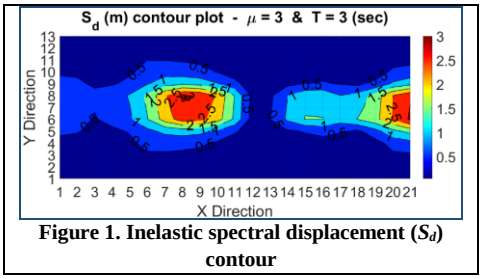

Figure 1. Inelastic spectral displacement (S_d) contour

3.2. Investigation of inelastic S_a values

For the purpose of investigating S_a in the inelastic constant ductility status, some contours were drawn for $\mu=2$ and $\mu=3$ statuses. By comparing these contours with elastic contour, it was specified that up to the period of 4sec, the maximum value occurred on the right side of the epicenter, and after the period of 4sec, the maximum value was observed on the left side. The location of the maximum value in low periods was similar in three statuses, and in high periods was approximately similar. By increasing μ the maximum value of S_a was decreased except for the period of 0.5sec. The location of the maximum value is constant for different periods. Figure 1 shows the inelastic spectral displacement (S_a) contour for fault-normal records (for the case μ=3).

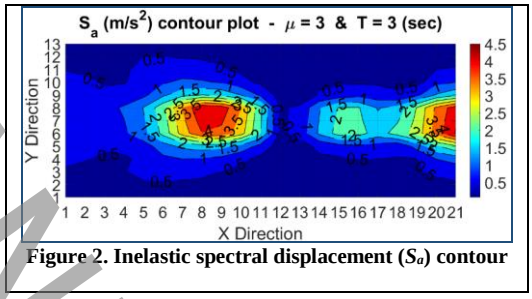

Figure 2. Inelastic spectral displacement (S_a) contour

3.3. Strong ground motion parameters

In the investigation of strong ground motion parameters (i.e. PGA, PGV, and PGD), it was observed that the maximum values happened in the end rows that coincides with the location of the maximum value of S_d and S_a. This means that in the regions where the maximum responses were observed, the intensity and the ground displacement were higher. Figure 3 demonstrates the variation of strong ground motion parameters versus fault alignment via colorful contours.

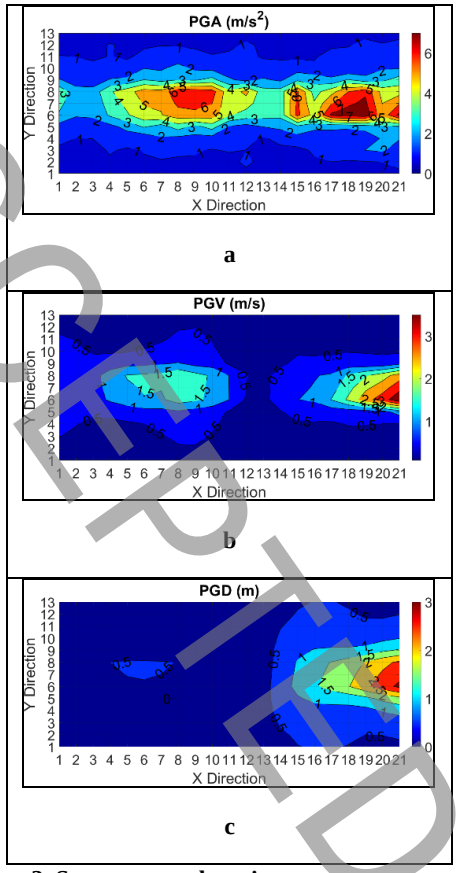

Figure 3. Strong ground motion parameters contours

4. Conclusions

- By comparing S_d and S_a in the forms of elastic and inelastic behavior for two ductility demand ratios ($\mu=2$ and $\mu=3$), approximately a similar trend was seen between elastic and inelastic responses. Therefore, by an appropriate approximation by elastic analysis, one can estimate the values of the maximum responses and the corresponding locations for inelastic behavior.
- Both parameters of R and θ (distance and angle from fault alignment) are important; two stations may have the same R but because of having different θ, different responses would be achieved.
- The Effect of *directivity* is slight on the low-period structures. But this effect is quite obvious in the response of long-period structures. So that in the period of 0.5sec, the diagram is seen as a line and in the period of 4sec, the diagram is seen as a parabola.

5. References

[1] Madhu Girija H, Gupta VK. Scaling of constant-ductility residual displacement spectrum. Earthquake Engineering & Structural Dynamics 2020;49:215–33.

[2] Hamidi H, Karbassi A, Lestuzzi P. Seismic response of RC buildings subjected to fling-step in the near-fault region. Structural Concrete 2020; 21(5).

[3] Liossatou E, Fardis MN. Near-fault effects on residual displacements of RC structures. Earthquake Engineering & Structural Dynamics 2016;45:1391–409.

[4] Khaloo AR, Khosravi H, Hamidi Jamnani H. Nonlinear interstory drift contours for idealized forward directivity pulses using "modified fish-bone" models. Advances in Structural Engineering 2015;18:603–27.

[5] Nievas CI, Sullivan TJ. Accounting for directionality as a function of structural typology in performance-based earthquake engineering design. Earthquake Engineering & Structural Dynamics 2017;46:791–809.

[6] Bradley BA, Baker JW. Ground motion directionality in the 2010–2011 Canterbury earthquakes. Earthquake Engineering & Structural Dynamics 2015;44:371–84.

[7] Nicknam A, Barkhodari MA, Hamidi Jamnani H, Hosseini A. Compatible seismogram simulation at near source site using Multi-Taper Spectral Analysis approach (MTSA). Journal of Vibroengineering 2013;15.

[8] Pinzón LA, Mánica MA, Pujades LG, Alva RE. Dynamic soil-structure interaction analyses considering directionality effects. Soil Dynamics and Earthquake Engineering 2020;130:106009.

[9] Grant DN, Padilla D, Greening PD. Orientation dependence of earthquake ground motion and structural response. Protection of Built Environment Against Earthquakes, Springer; 2011, p. 57–73.

[10] Hamidi H, Khosravi H, Soleimani R. Fling-step ground motions simulation using theoretical-based Green's function technique for structural analysis. Soil Dynamics and Earthquake Engineering 2018;115:232–45.

[11] Abrahamson N. Seismological aspects of near-fault ground motions. 5th Caltrans Seismic Research Workshop, 1998.

[12] Heaton TH, Hall JF, Wald DJ, Halling MW. Response of high-rise and base-isolated buildings to a hypothetical Mw 7.0 blind thrust earthquake. Science 1995;267:206.

[13] Somerville PG. Development of ground motion time histories for phase 2 of the FEMA/SAC steel project. SAC Joint Venture; 1997.

[14] ASCE-7. Minimum Design Loads and Associated Criteria for Buildings and Other Structures. ASCE/SEI 7-16; 2016.

↑ please level both columns of the last page as far as possible. ↑